photonics

MDPI

Communication

Geometric Visualization of the 3D Polarimetric Information of an Arbitrary Electromagnetic Field

Yahong Li [1], Bosong Li [1], Wenhao Wei [1], Xiangwei Zeng [2], Yuegang Fu [3] and Yu Zhao [4,*]

1 Research Institute of Photonics, Dalian Polytechnic University, Dalian 116034, China; liyahong@dlpu.edu.cn (Y.L.); lbs1230@outlook.com (B.L.); wwenhao0308@outlook.com (W.W.)
2 College of Transportation, Ludong University, Yantai 264025, China; zeng3876@ldu.edu.cn
3 School of Opto−Electronic Engineering, Changchun University of Science and Technology, Changchun 130022, China; fuyg@cust.edu.cn
4 Changchun Institute of Optics, Fine Mechanics and Physics, Chinese Academy of Sciences, Changchun 130033, China
* Correspondence: zhaoyu@ciomp.ac.cn

Abstract: The geometric visualization in this study concerns the three−dimensional (3D) polarimetric information of an arbitrary electromagnetic field. Based on previous research, a 3 × 3 coherency matrix $\mathbf{\Phi}$ can be decomposed into an incoherent superposition of a totally 3D−polarized component $\mathbf{\Phi}_{3D\_p}$, a specific partially 3D−polarized component $\mathbf{\Phi}_{3D\_pp}$ with a 3D degree of polarization (DoP) of 1/2, and a totally 3D−unpolarized component $\mathbf{\Phi}_{3D\_up}$. Combining the physical meaning of this decomposition, we mathematically construct three polarization purities, namely, P_{3D_p}, P_{3D_pp}, and P_{3D_up}, for an arbitrary electromagnetic field to quantify the weight of the three 3D−polarized components. In order to show the proportion of the three polarized components of an electromagnetic field intuitively, we propose a geometric representation of a spatially quadric surface. Finally, two examples are cited to demonstrate the applicability of intuitively displaying the 3D polarimetric information of an arbitrary electromagnetic field.

Keywords: polarimetry; electromagnetic field; 3D polarization; degree of polarization

check for updates

Citation: Li, Y.; Li, B.; Wei, W.; Zeng, X.; Fu, Y.; Zhao, Y. Geometric Visualization of the 3D Polarimetric Information of an Arbitrary Electromagnetic Field. *Photonics* **2023**, *10*, 1040. https://doi.org/10.3390/photonics10091040

Received: 27 June 2023
Revised: 3 September 2023
Accepted: 5 September 2023
Published: 12 September 2023

1. Introduction

Recently, ellipsometry and polarimetry have become of topical interest in respect of statistical electromagnetic fields [1–6]. In 3D polarization cases, the usual 2D mathematical and geometric representations of polarization are not available [7–10]. This necessitates the introduction of appropriate representations to characterize the polarization properties of statistical electromagnetic fields. One important physical quantity is the 3D degree of polarization (DoP) for statistical electromagnetic fields. The concept of the DoP was first introduced by Samson [11], and it was developed by Barakat [12], T. Setälä [13], and José J. Gil et al. [14]. Now, the definition of the DoP has been accepted to mean that two parameters are needed for specifying a random statistical electromagnetic field, i.e., the indices of polarimetric purity (P1, P2) named by José J. Gil [15–17]. Based on the definition of the DoP, Colin J. R. Sheppard and José J. Gil proposed geometric representations of the DoP in terms of a triangular composition plot [10] and a polarimetric purity space [15,16]. However, there is still more to learn about representations that can intuitively express the DoP. The main aim of this article is, based on the above−mentioned parameters (P1, P2), to introduce a completely different geometric representation. Using the intrinsic relationship between the DoP and the three defined parameters, a spatially quadric surface is depicted to quantify the 3D polarimetric information of a statistical electromagnetic field.

2. Methods

Given a point $\boldsymbol{r}$ in a 3D space {xyz} at time t, the electric field vector $\mathbf{E}(\boldsymbol{r}, t)$ of a random electromagnetic field can be written as the 3 × 1 complex vector, i.e., the 3D instantaneous Jones vector [15],

$$\mathbf{E}(\boldsymbol{r},t)=\begin{pmatrix}E_x(\boldsymbol{r},t)\\E_y(\boldsymbol{r},t)\\E_z(\boldsymbol{r},t)\end{pmatrix}=\begin{pmatrix}A_x(\boldsymbol{r},t)\\A_y(\boldsymbol{r},t)e^{i(\delta_y(\boldsymbol{r},t)-\delta_x(\boldsymbol{r},t))}\\A_z(\boldsymbol{r},t)e^{i(\delta_z(\boldsymbol{r},t)-\delta_x(\boldsymbol{r},t))}\end{pmatrix}\tag{1}$$

where $E_j(\boldsymbol{r},t)$ (j = x,y,z) are the three orthogonal electric field components of the electric field vector in a space coordinate system {xyz}, $A_j(\boldsymbol{r},t)$ (j = x,y,z) are the amplitudes of three electric field components, and $\delta_j(\boldsymbol{r},t)$ (j = x,y,z) are the phases of three electric field components.

The polarization properties of a random electromagnetic field are expressed by a 3 × 3 coherency matrix [17], which is defined as

$$\boldsymbol{\Phi}=\begin{pmatrix}\langle E_x(\boldsymbol{r},t)\cdot E_x^*(\boldsymbol{r},t)\rangle & \langle E_x(\boldsymbol{r},t)\cdot E_y^*(\boldsymbol{r},t)\rangle & \langle E_x(\boldsymbol{r},t)\cdot E_z^*(\boldsymbol{r},t)\rangle\\ \langle E_y(\boldsymbol{r},t)\cdot E_x^*(\boldsymbol{r},t)\rangle & \langle E_y(\boldsymbol{r},t)\cdot E_y^*(\boldsymbol{r},t)\rangle & \langle E_y(\boldsymbol{r},t)\cdot E_z^*(\boldsymbol{r},t)\rangle\\ \langle E_z(\boldsymbol{r},t)\cdot E_x^*(\boldsymbol{r},t)\rangle & \langle E_z(\boldsymbol{r},t)\cdot E_y^*(\boldsymbol{r},t)\rangle & \langle E_z(\boldsymbol{r},t)\cdot E_z^*(\boldsymbol{r},t)\rangle\end{pmatrix}=\begin{pmatrix}\phi_{xx} & \phi_{xy} & \phi_{xz}\\ \phi_{yx} & \phi_{yy} & \phi_{yz}\\ \phi_{zx} & \phi_{zy} & \phi_{zz}\end{pmatrix}\tag{2}$$

From the perspective of polarimetry (to measure the intensity values of different polarized components), similar to 2D polarization, the 3D polarimetry [18,19] is often expressed in the form of the 9 × 1 Stokes vector $\mathbf{S}_{9\times1}$,

$$\mathbf{S}_{9\times1}=(s_0,s_1,s_2,s_3,s_4,s_5,s_6,s_7,s_8)^T\tag{3}$$

where the first parameter s_0 is the total intensity of the 3D electromagnetic field, and the others, s_j (j = 1, 2, . . ., 8), are the intensity values of specific polarized components of the 3D electromagnetic field, in which the specific polarized directions are determined by eight 3 × 3 Gell–Mann matrices [20] plus a 3 × 3 identity matrix.

Regarding how to derive the 3 × 3 coherence matrix $\boldsymbol{\Phi}$ or 9 × 1 Stokes vector $\mathbf{S}_{9\times1}$ from a 3 × 1 electric field vector $\mathbf{E}(\boldsymbol{r},t)$, the theoretical derivations have been published in Ref. [7]. Using a particular 3 × 3 matrix basis composed of eight linearly independent 3 × 3 Gell–Mann matrices [20] plus the 3 × 3 identity matrix, an inherent transformation relationship between the elements of 3 × 3 coherence matrix $\boldsymbol{\Phi}$ and 9 × 1 Stokes vector $\mathbf{S}_{9\times1}$ can be expressed by

$$\boldsymbol{\Phi}=\begin{pmatrix}\frac{1}{2}s_3+\frac{\sqrt{6}}{6}s_0+\frac{\sqrt{3}}{6}s_8 & \frac{1}{2}(s_1-i\cdot s_2) & \frac{1}{2}(s_4-i\cdot s_5)\\ \frac{1}{2}(s_1+i\cdot s_2) & \frac{\sqrt{6}}{6}s_0+\frac{\sqrt{3}}{6}s_8-\frac{1}{2}s_3 & \frac{1}{2}(s_6-i\cdot s_7)\\ \frac{1}{2}(s_4+i\cdot s_5) & \frac{1}{2}(s_6+i\cdot s_7) & \frac{\sqrt{6}}{6}s_0-\frac{\sqrt{3}}{3}s_8\end{pmatrix}\tag{4}$$

$$\begin{cases} s_0=\frac{\sqrt{6}}{3}(\phi_{xx}+\phi_{yy}+\phi_{zz}) & s_1=\phi_{xy}+\phi_{yx} & s_2=(\phi_{xy}-\phi_{yx})i\\ s_3=\phi_{xx}-\phi_{yy} & s_4=\phi_{xz}+\phi_{zx} & s_5=(\phi_{xz}-\phi_{zx})i\\ s_6=\phi_{yz}+\phi_{zy} & s_7=(\phi_{yz}-\phi_{zy})i & s_8=\frac{\sqrt{3}}{3}(\phi_{xx}+\phi_{yy}-2\phi_{zz})\end{cases}\tag{5}$$

where the symbol i indicates an imaginary number.ϕ_{mn}(m, n = x, y, z) are the elements of the 3 × 3 coherence matrix. s_j (j = 0, 1, . . ., 8) are the corresponding nine Stokes parameters.

Obviously, the nine Stokes parameters are all measurable, real values. The physical meanings of the nine Stokes parameters are as shown in Table 1 below. It is noted that the constant coefficients of each Stokes parameter are determined by the properties of a particular 3 × 3 matrix basis [7], and they have no specific physical meaning.

Table 1. Physical meanings of the 3D Stokes parameters.

Stokes Parameters	Physical Meanings
s_0	Total intensity
s_1	Sum of intensities of $\pm 45^\circ$ polarized components in x–y plane
s_2	Difference in intensities of left/right−handed circular polarized components in x–y plane
s_3	Difference in intensities between the x and y polarized components
s_4	Sum of intensities of $\pm 45^\circ$ polarized components in x–z plane
s_5	Difference in intensities of left/right−handed circular polarized components in x–z plane
s_6	Sum of intensities of $\pm 45^\circ$ polarized components in y–z plane
s_7	Difference in intensities of left/right−handed circular polarized components in y–z plane
s_8	Sum of differences in intensities between the x and y polarized components and the z polarized component, respectively.

In order to better analyze the polarimetric information of the measured 3D electromagnetic field, we decompose the 3×3 coherency matrix shown in Equation (4) into an incoherent superposition of a totally 3D−polarized component $\mathbf{\Phi}_{3D\_p}$, a specific 3D partially polarized component $\mathbf{\Phi}_{3D\_pp}$, and a totally 3D−unpolarized component $\mathbf{\Phi}_{3D\_up}$. The DoP values of the three 3D−polarized components are 1, 0.5, and 0, respectively. The decomposition result of the 3×3 coherency matrix can be expressed as

$$\mathbf{\Phi} = \mathrm{I}_{3D-p} \cdot \mathbf{\Phi}_{3D-p} + \mathrm{I}_{3D-pp} \cdot \mathbf{\Phi}_{3D-pp} + \mathrm{I}_{3D-up} \cdot \mathbf{\Phi}_{3D-up} \tag{6}$$

$$\begin{cases} \mathbf{\Phi} = (\boldsymbol{\nu}_1\boldsymbol{\nu}_2\boldsymbol{\nu}_3) \cdot Diag(\lambda_1, \lambda_2, \lambda_3) \cdot (\boldsymbol{\nu}_1\boldsymbol{\nu}_2\boldsymbol{\nu}_3)^\dagger, \lambda_1 \geq \lambda_2 \geq \lambda_3 \geq 0 \\ \mathrm{I}_{3D-P} = \lambda_1 - \lambda_2, \mathbf{\Phi}_{3D-p} = (\boldsymbol{\nu}_1\boldsymbol{\nu}_2\boldsymbol{\nu}_3) \cdot \begin{pmatrix} tr(\mathbf{\Phi}) & 0 & 0 \\ 0 & 0 & 0 \\ 0 & 0 & 0 \end{pmatrix} \cdot (\boldsymbol{\nu}_1\boldsymbol{\nu}_2\boldsymbol{\nu}_3)^\dagger \\ \mathrm{I}_{3D-pp} = \lambda_2 - \lambda_3, \mathbf{\Phi}_{3D-pp} = (\boldsymbol{\nu}_1\boldsymbol{\nu}_2\boldsymbol{\nu}_3) \cdot \begin{pmatrix} tr(\mathbf{\Phi}) & 0 & 0 \\ 0 & tr(\mathbf{\Phi}) & 0 \\ 0 & 0 & 0 \end{pmatrix} \cdot (\boldsymbol{\nu}_1\boldsymbol{\nu}_2\boldsymbol{\nu}_3)^\dagger \\ \mathrm{I}_{3D-up} = \lambda_3, \mathbf{\Phi}_{3D-up} = (\boldsymbol{\nu}_1\boldsymbol{\nu}_2\boldsymbol{\nu}_3) \cdot \begin{pmatrix} tr(\mathbf{\Phi}) & 0 & 0 \\ 0 & tr(\mathbf{\Phi}) & 0 \\ 0 & 0 & tr(\mathbf{\Phi}) \end{pmatrix} \cdot (\boldsymbol{\nu}_1\boldsymbol{\nu}_2\boldsymbol{\nu}_3)^\dagger \end{cases} \tag{7}$$

where λ_j and $\boldsymbol{\nu}_j$ $(j = 1, 2, 3)$ are the eigenvalues and eigenvectors of the 3×3 coherency matrix. The subscripts $_{3D-p}$, $_{3D-pp}$, and $_{3D-up}$ represent the 3D totally polarized component, 3D partially polarized component, and 3D totally unpolarized component, respectively. I_{3D-p}, I_{3D-pp}, and I_{3D-up} are the corresponding weight values. $\mathbf{\Phi}_{3D-p}$, $\mathbf{\Phi}_{3D-pp}$, and $\mathbf{\Phi}_{3D-up}$ are the 3×3 coherency matrices of the three 3D−polarized components. The symbol † represents the complex conjugate transpose.

The above decomposition method included in Equations (5) and (6) has also been mentioned in several papers [15–17], and it is referred to as characteristic or trivial decomposition. In some papers [1,15], the second term $\mathbf{\Phi}_{3D-pp}$ with a DoP of 0.5 is defined as a 2D−unpolarized component, but this is not always true. A detailed discussion of this explanation will be included in the last two examples. To quantify the weight of the three decomposed polarized components in the measured 3D electromagnetic field, we redefine three polarization purities

$$\begin{cases} P_{3D-p} = \frac{I_{3D-p}}{I_{Total}} = \frac{\lambda_1-\lambda_2}{\lambda_1+\lambda_2+\lambda_3} \\ P_{3D-pp} = \frac{I_{3D-pp}}{I_{Total}} = \frac{2(\lambda_2-\lambda_3)}{\lambda_1+\lambda_2+\lambda_3} \\ P_{3D-up} = \frac{I_{3D-up}}{I_{Total}} = \frac{3\lambda_3}{\lambda_1+\lambda_2+\lambda_3} \end{cases} \tag{8}$$

where $I_{Total} = tr(\mathbf{\Phi}) = \lambda_1 + \lambda_2 + \lambda_3$ is the total intensity of the measured 3D electromagnetic field.

Obviously, the value ranges of the three polarization purities are between 0 and 1, and they are always satisfied with the identical equation,

$$P_{3D-p} + P_{3D-pp} + P_{3D-up} = 1 \tag{9}$$

In the literature [15,16], José J. Gil defines $P_1 = P_{3D\_p}$ as the degree of purity, and $P_2 = 1-P_{3D\_up}$ is defined as the degree of directionality. We combine with the DoP for the 3D electromagnetic field defined in the literature [3,4], the relationship among the redefined three polarization purities shown in Equation (8), and the DoP is derived as follows:

$$DoP^2 = P_{3D-p}^2 + \frac{1}{2}P_{3D-p} \cdot P_{3D-pp} + \frac{1}{4}P_{3D-pp}^2 \tag{10}$$

Combined with the inequality of the arithmetic and geometric means and Equation (9), the three polarization purities fulfill the following two inequations:

$$\begin{cases} \frac{1}{3}(P_{3D-p} + P_{3D-pp} + P_{3D-up})^2 \le P_{3D-p}^2 + P_{3D-pp}^2 + P_{3D-up}^2 \le (P_{3D-p} + P_{3D-pp} + P_{3D-up})^2 \\ \frac{1}{3} \le P_{3D-p}^2 + P_{3D-pp}^2 + P_{3D-up}^2 \le 1 \end{cases} \tag{11}$$

3. Results

Using the above three polarization purities P_{3D-p}, P_{3D-pp}, and P_{3D-up} defined in Equation (8) and the relationship shown in Equation (10), a spatially quadric surface is depicted, as shown in Figure 1. The x−axis corresponds to P_{3D-p}, the y−axis corresponds to P_{3D-pp}, and the z−axis corresponds to the DoP. The side views of the three orthogonal directions of the spatially quadric surface are also shown in subgraphs (a–c) in Figure 1.

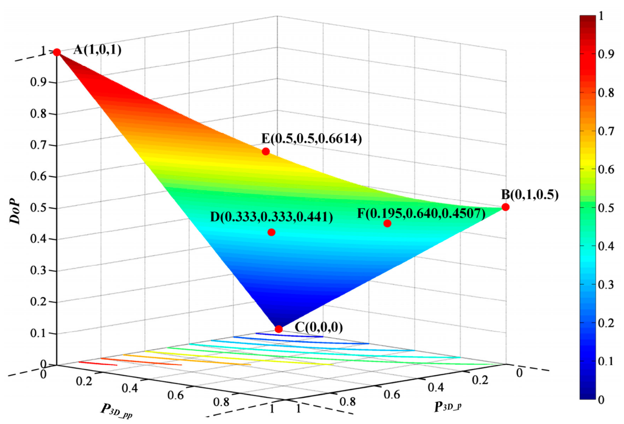

Figure 1. *Cont.*

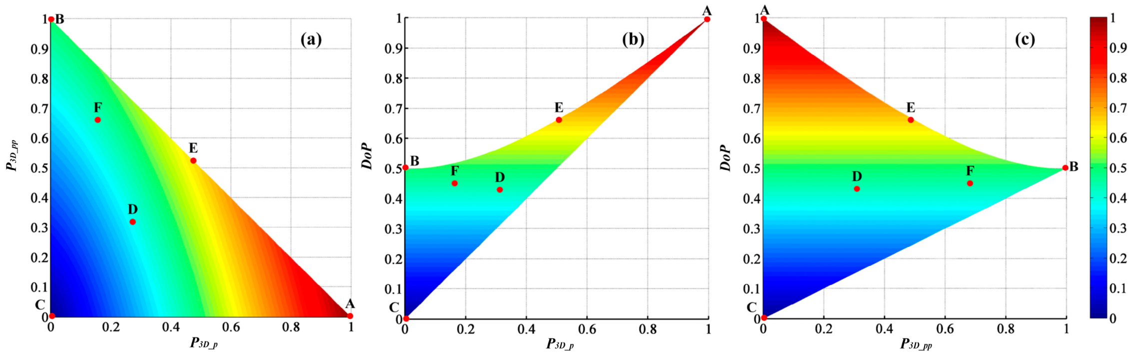

Figure 1. The spatially quadric surface is constructed to display the 3D polarimetric result of the DoP, in which the x−axis, y−axis, and z−axis correspond to the three polarization purities P_{3D-p}, P_{3D-pp}, and DoP. The subgraphs (**a**–**c**) are the orthogonal 2D projections of the spatially quadric surface on the (**a**) x−y plane, (**b**) x−z plane, and (**c**) y−z plane.

4. Discussion

In this section, we mainly discuss the 3D polarimetric information corresponding to some special points on the spatially quadric surface. When the right−hand inequation in Equation (11) takes the equal sign, the values of P_{3D-p}, P_{3D-pp}, and P_{3D-up} are satisfied with the condition that $P_{3D-p} = P_{3D-pp} = P_{3D-up} = 0.3333$. This special case means it is completely possible for electromagnetic fields to occur during 3D polarimetry. Combined with Equation (10), it is verified that this special case corresponds to a 3D partially polarized field with a DoP of 0.4410. Hence, it is concluded that only one point on the quadric surface is feasible, shown as point D (0.3333, 0.3333, 0.4410) in Figure 1. The value of the DoP is determined by the color of the location of point D, not the color of point D itself.

Similarly, the equal sign of the left−hand inequation in Equation (11) holds if, and only if, one of P_{3D-p}, P_{3D-pp}, and P_{3D-up} is equal to 1. According to Equation (10), the three cases characterize the totally polarized field, partially polarized field, and totally un−polarized field in 3D space, respectively. The corresponding values of the DoP are 1, 0.5, and 0. Therefore, the polarimetric results of these three cases are represented by three different points, i.e., points A (1, 0, 0), B (0, 1, 0), and C (0, 0, 1), as shown in Figure 1. The colors of the positions of the three points, i.e., red, light green, and blue, indicate that the values of the DoP are 1, 0.5, and 0. Hence, there are three special points on the quadric surface. It is worth emphasizing that all points that will fall in the quadric surface are always physically reachable.

Next, we take two general electromagnetic fields as examples to demonstrate the applicability and validity of the proposed geometric visualization shown in Figure 1. A hig numerical aperture (NA) microscope objective (NA = 1.25 immersed in oil) with anti−reflective (AR) coatings is introduced; the parameters of the optical system are shown in Table 2. The transmittance curve and phase−shift curve corresponding to the multilayer dielectric AR coating are shown in Figure 2.

Table 2. Optical parameters of a high NA microscope objective.

Amplification factor	100×
Numerical aperture (NA)	1.25
Object height/mm	0.11
Working wavelength/nm	486~656
Total length/mm	315.66
Effective working distance/mm	0.42
Back working distance/mm	199.447

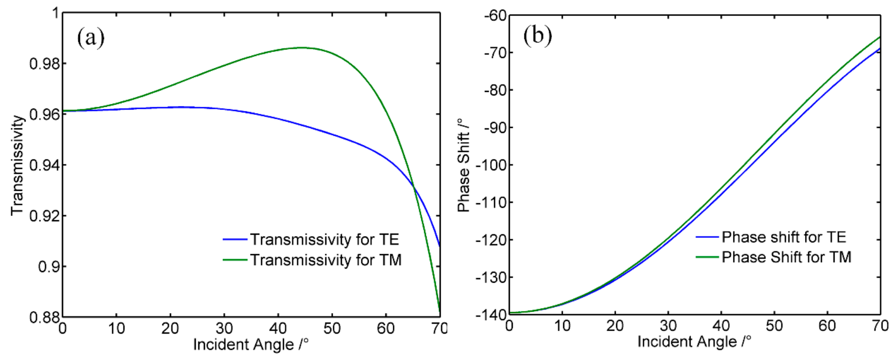

Figure 2. Transmissivity and phase shift of the multilayer dielectric AR coating, the subgraphs (**a**,**b**) represent the relationship curves between transmissivity and phase shift of TE mode and TM mode and incidence angle of the multilayer dielectric AR coating, respectively.

When the incident light is 3D partially polarized light, the corresponding 3D coherency matrix is

$$\mathbf{\Phi}_{in} = \begin{pmatrix} 1 & 0 & 0 \\ 0 & 1 & 0 \\ 0 & 0 & 0 \end{pmatrix} \tag{12}$$

The field of view (FoV) of the system is given in the form of the object height h = 0.11 mm. Based on the proposed 3D polarization algebra [7], the polarization ray tracing of the partially polarized light incident optical system can be completed. Since the paths of each sampled ray in the optical system are not equal, the polarization transformation effects of each sampled ray are not the same. Here, we arbitrarily choose the two exampled rays at the exit pupil, and the 3 × 3 coherency matrices can be calculated as follows:

$$\mathbf{\Phi}(\mathrm{E}) == \begin{pmatrix} 0.5 & -0.25i & 0 \\ 0.25i & 0.5 & 0 \\ 0 & 0 & 0 \end{pmatrix} \mathbf{\Phi}(\mathrm{F}) = \begin{pmatrix} 0.25 & 0.125 & 0.125i \\ 0.125 & 0.5 & -0.125i \\ -0.125i & 0.125i & 0.25 \end{pmatrix} \tag{13}$$

Firstly, we make the characteristic decompositions of the above 3 × 3 coherency matrices included in Equation (7). Then, we apply the decomposition results to Equations (8)–(10), and the polarimetric results of the two exampled rays are determined by points E (0.5, 0.5, 0.6614) and F (0.1952, 0.6404, 0.4507), which are located in the quadric surface shown in Figure 1. Therefore, the two exampled rays are 3D partially polarized fields, and the colors of position E and position F depend on the values of the DoP, i.e., orange and green, respectively.

Last but not least, we examine the second items $\mathbf{\Phi}_{\mathrm{3D-pp}}(\mathrm{E})$ and $\mathbf{\Phi}_{\mathrm{3D-pp}}(\mathrm{F})$ in the characteristic decomposition results of these two examples included in Equation (13),

$$\mathbf{\Phi}_{\mathrm{3D-pp}}(\mathrm{E}) == \begin{pmatrix} 1 & 0 & 0 \\ 0 & 1 & 0 \\ 0 & 0 & 0 \end{pmatrix}, \mathbf{\Phi}_{\mathrm{3D-pp}}(\mathrm{F}) = \begin{pmatrix} 0.5681 & 0.2425 & 0.4319i \\ 0.2425 & 0.8638 & -0.2425i \\ -0.4319i & 0.2425i & 0.5681 \end{pmatrix} \tag{14}$$

Obviously, $\mathbf{\Phi}_{\mathrm{3D-pp}}(\mathrm{E})$ is a 2D totally unpolarized field, but $\mathbf{\Phi}_{\mathrm{3D-pp}}(\mathrm{F})$ is a 3D partially polarized field with a DoP of 1/2. Combined with Equation (13), the first exampled 3D electromagnetic field does not contain a z−component, i.e., the vibration directions at a point are statistically in a constant 2D x–y plane at different times. However, the vibration direction of the second exampled 3D electromagnetic field fluctuates in 3D space, so the second polarized component is no longer 2D unpolarized.

5. Conclusions

On the basis of previous research, we redefined the three polarization purities via the characteristic decomposition of a 3 × 3 coherency matrix. Combined with the definition of the 3D DoP, we mathematically explored the relationships between the three polarization purities and the 3D DoP. Then, the geometric visualization of a quadric surface was constructed to quantify the 3D polarimetric information of an arbitrary electromagnetic field. It is useful for 3D polarimetry to intuitively display the polarization properties of the measured electromagnetic field, and this is also expected to be of application in near−field optics, singular optics, and nanophotonics.

Author Contributions: Conceptualization, X.Z.; methodology, Y.L.; formal analysis, B.L. and W.W.; data curation, Y.Z.; writing—original draft preparation, Y.Z. and Y.F.; writing—review and editing, X.Z. and Y.L. All authors have read and agreed to the published version of the manuscript.

Funding: This research was funded by the National Natural Science Foundation of China (NSFC), grant numbers 11904044 and 62105136.

Institutional Review Board Statement: Not applicable.

Informed Consent Statement: Not applicable.

Data Availability Statement: Data underlying the results presented in this paper are not publicly available at this time but can be obtained from the authors upon reasonable request.

Acknowledgments: The authors would like to thank Peter J. Bryanston−Cross from the school of engineering, university of Warwick for his full assistance.

Conflicts of Interest: The authors declare no conflict of interest.

References

1. Ellis, J.; Dogariu, A.; Ponomarenko, S.; Wolf, E. Degree of polarization of statistically stationary electromagnetic fields. *Opt. Commun.* **2005**, *248*, 333–337. [CrossRef]
2. Dennis, M.R. A three−dimensional degree of polarization based on Rayleigh scattering. *J. Opt. Soc. Am. A* **2007**, *24*, 2065–2074. [CrossRef] [PubMed]
3. Setälä, T.; Lindfors, K.; Friberg, A.T. Degree of polarization for in 3D optical fields generated from a partially polarized plane wave. *Opt. Lett.* **2009**, *34*, 3394–3397. [CrossRef] [PubMed]
4. Gil, J.J. Interpretation of the coherency matrix for three−dimensional polarization states. *Phys. Rev. A* **2014**, *90*, 043858–043877. [CrossRef]
5. Azzam, R.M.A. Three−dimensional polarization states of monochromatic light fields. *J. Opt. Soc. Am. A* **2011**, *28*, 2279–2285. [CrossRef] [PubMed]
6. Voipio, T.; Setälä, T.; Shevchenko, A.; Friberg, A.T. Polarization dynamics and polarization time of random three−dimensional electromagnetic fields. *Phys. Rev. A* **2010**, *82*, 239–241. [CrossRef]
7. Li, Y.; Fu, Y.; Liu, Z.; Zhou, J.; Bryanston−Cross, P.J.; Li, Y.; He, W. Three−dimensional polarization algebra for all polarization sensitive optical systems. *Opt. Express* **2018**, *11*, 14109–14122. [CrossRef] [PubMed]
8. Sheppard, C.J.R.; Castello, M.; Diaspro, A. Three−dimensional polarization algebra. *J. Opt. Soc. Am. A* **2016**, *33*, 1938–1947. [CrossRef] [PubMed]
9. Dennis, M.R. Geometric interpretation of the three−dimensional coherence matrix for nonparaxial polarization. *J. Opt. A Pure Appl. Opt.* **2004**, *6*, S26–S31. [CrossRef]
10. Sheppard, C.J. Geometric representation for partial polarization in three dimensions. *Opt. Lett.* **2012**, *37*, 2772–2774. [CrossRef] [PubMed]
11. Samson, J.C. Descriptions of the polarization states of vector processes: Applications to ULF magnetic fields. *Geophys. J. R. Astron. Soc.* **1973**, *34*, 403–419. [CrossRef]
12. Barakat, R. Degree of polarization and the principal idempotents of the coherency matrix. *Opt. Commun.* **1977**, *23*, 147–150. [CrossRef]
13. Setälä, T.; Shevchenko, A.; Kaivola, M.; Friberg, A.T. Degree of polarization for optical near fields. *Phys. Rev.* **2002**, *66*, 016615–016622. [CrossRef] [PubMed]
14. Gil, J.J.; Norrman, A.; Friberg, A.T.; Setälä, T. Polarimetric purity and the concept of degree of polarization. *Phys. Rev. A* **2018**, *97*, 023838–023842. [CrossRef]
15. Gil, J.J. Polarimetric characterization of light and media: Physical quantities involved in polarimetric phenomena. *Eur. Phys. J. Appl. Phys.* **2007**, *40*, 1–47. [CrossRef]
16. Gil, J.J.; San José, I. 3D polarimetric purity. *Opt. Commun.* **2010**, *283*, 4430–4434. [CrossRef]

17. Gil, J.J.; Friberg, A.T.; Setälä, T. Structure of polarimetric purity of three−dimensional polarization states. *Phys. Rev. A* **2017**, *95*, 053856–053865. [CrossRef]
18. Ellis, J.; Dogariu, A. Optical polarimetry of random fields. *Phys. Rev. Lett.* **2005**, *95*, 203905–203908. [CrossRef] [PubMed]
19. Leppänen, L.-P.; Friberg, A.T.; Setälä, T. Partial polarization of optical beams and near fields probed with a nanoscatterer. *J. Opt. Soc. Am. A* **2014**, *31*, 1627–1635. [CrossRef]
20. Gell-Mann, M. Symmetries of Baryons and Mesons, Murray Gell-Mann. *Phys. Rev.* **1962**, *125*, 1067–1084. [CrossRef]